

Molecular BioSystems

Accepted Manuscript



This is an *Accepted Manuscript*, which has been through the Royal Society of Chemistry peer review process and has been accepted for publication.

Accepted Manuscripts are published online shortly after acceptance, before technical editing, formatting and proof reading. Using this free service, authors can make their results available to the community, in citable form, before we publish the edited article. We will replace this *Accepted Manuscript* with the edited and formatted *Advance Article* as soon as it is available.

You can find more information about *Accepted Manuscripts* in the [Information for Authors](#).

Please note that technical editing may introduce minor changes to the text and/or graphics, which may alter content. The journal's standard [Terms & Conditions](#) and the [Ethical guidelines](#) still apply. In no event shall the Royal Society of Chemistry be held responsible for any errors or omissions in this *Accepted Manuscript* or any consequences arising from the use of any information it contains.



www.rsc.org/molecularbiosystems

Live cell interactome of the human Voltage Dependent Anion Channel 3 (VDAC3) revealed in HeLa cells by Affinity Purification Tag Technique

Angela Messina^{1,2, *}, Simona Reina^{1,2}, Francesca Guarino^{1,2}, Andrea Magri^{1,2}, Flora Tomasello^{1,2}, Richard E. Clark³, Rona R. Ramsay³ and Vito De Pinto^{1,2}

¹ Department of Biological, Geological and Environmental Sciences, Section of Molecular Biology, University of Catania, Italy

² National Institute for Biomembranes and Biosystems, Section of Catania, viale A. Doria 6, 95125 Catania, Italy

³ Biomedical Sciences Research Complex, School of Biology, University of St Andrews, Biomedical Science Building, North Haugh, St Andrews, Fife KY16 9ST, UK

* corresponding author: mess@unict.it

Running title: Interactome of VDAC3

Correspondence to:

dr. Angela Messina
Department of Biological, Geological and Environmental Sciences
Section of Molecular Biology,
University of Catania
Building 2, floor 3
CU S.Sofia, viale A. Doria, 6
95125 Catania, ITALY
tel: +39 095 7384231
e-mail: mess@unict.it

ABSTRACT

In higher eukaryotes three different VDAC genes encode three homologous proteins which do not show the same activity. VDAC1 and VDAC2 isoforms have been characterized while VDAC3 isoform is still elusive. To explore VDAC3 protein interactions, we have established a stable cell line expressing a fluorescent and dual-tagged construct. This clone expresses a stable amount of VDAC3. Live cell imaging shows that fluorescent VDAC3 localizes in the mitochondria. Proteins interacting with VDAC3 have been separated by tandem-affinity purification and 2-D gel electrophoresis and identified by mass spectrometry. In the list of putative interacting proteins, there are cytosolic, mitochondrial, cytoskeletal and ER proteins. Coherent pathways like cell redox homeostasis, response to stress, formation/rearrangement of disulfide bonds, response to unfolded proteins or protein folding have been found to be related to clusters of proteins identified in this experiment. The list of associated proteins has been validated by immunoprecipitation experiments utilizing specific antibodies. Likely biological and pathological processes have been analyzed. Cytosolic proteins associated with VDAC3 include tubulins and cytoskeletal proteins, stress sensors, chaperones and proteasome components, redox-mediating enzymes such as protein disulphide isomerase. The overall picture points to a role for VDAC3 as mediator for the organization of protein complexes and regulator of the traffic of misfolded or non-folded proteins evoked from different stimuli.

1. Introduction

The voltage-dependent anion channel (VDAC) is a small family of integral membrane proteins of the outer mitochondrial membrane (OMM) whose role is to allow the flow of hydrophilic metabolites such as substrates, ATP and ADP between the mitochondrion and the cytosol [1-3]. The most abundant member of this family is VDAC1, and its abundance is probably why most of the information accumulated in the last thirty years is about this isoform. The functional features of VDAC1 are well characterized [1-3], and, furthermore, it has been implicated as an important factor in cell processes including apoptosis [4-5], calcium homeostasis [6] and diseases such as cancer [7]. Deficiency of VDAC1 has been associated with a lethal encephalomyopathy [8]. The intensive research culminated in the proposal of the 3D structure by different groups almost in the same time [9-12]. The topology of the protein in the membrane has been determined [13].

Three different VDAC isoforms have been characterized in higher eukaryotes, encoded by three separate genes [14-15]. The relative abundance of the isoforms has been assayed in HeLa cells where VDAC1 is ten and one hundred times more prevalent than VDAC2 and VDAC3, respectively [14]. The amino acid sequence of human isoforms (hVDAC) are 68% to 75% pairwise identical, with 80-90% overall similarity. Predicted secondary structure is also similar [15], and homology modelling simulations show that VDAC2 and VDAC3 are presumably arranged in the membrane in the same way as VDAC1 [13-15].

It is of general interest to evaluate the meaning of the presence of three different VDAC isoforms in the cell, considering that they are ubiquitously expressed. VDAC3 is considered the more elusive component of the family because of its relatively low abundance [14] and because it behaves differently from the other isoforms in functional assays [16-17]. In a recent experiment of domain swapping among the three isoforms, VDAC3 was found to be able to form large pores only when its structure was changed [17-18]. Furthermore its cysteine residues are suspected to play a role in ROS control [17]. Following the production of knock-out mice deficient in VDAC3 [19], several observations pointed out a possible role of VDAC3 as a contact site or an organizational mediator for structural components of the cell like centrioles [20], outer dense fibers [21], and axoneme [19]. Mice lacking VDAC3 were indeed found to be healthy, but males are infertile because an axoneme disorganization [19].

A more careful consideration of VDAC3 function(s) is an urgent task and identification of any interaction partners would greatly aid understanding its cell function.

Interactomes can be defined as the context-dependent sets of interacting proteins. Finding these interaction partners and the interacting epitopes is crucial to the study of cellular functions, with obvious consequences for cell pathophysiology and technological applications. Interactoming

studies have been devised, and established techniques are used to obtain such lists of candidate interactors. The most known approach, the two-hybrid yeast system has largely been used, mainly for soluble proteins. When coming to the study of “Interactome” of membrane proteins, many technical problems arise. A main problem is the hydrophobic nature of the subject. This means that cellular interactors have to be considered in the frame of a membrane associated environment. Another pitfall, that makes “interactomic” an highly uncertain science, is the artificial situation created by extraction or solubilization with detergents or chaotropic agents, able to destroy the cellular environment.

In this work we present our results obtained with the application of a strategy respectful of the intracellular membrane localization of VDAC3. This aim was pursued by constructing a double-tagged VDAC3, and following a LAP-tag protocol (Localization and Affinity Purification tag), which combines the advantages of monitoring in living cells the localization of a fluorescent-tagged protein with the aid of the TAP-tag purification [22]. As a result, a list of interactors has been produced and examined for cellular consequences.

2. MATERIALS AND METHODS

2.1. Generation of the pEFIRES-YFP-TEV-6His-hVDAC3 construct.

The cDNA for the human VDAC3 (hVDAC3) was cloned SmaI/SalI in pQE30 (Qiagen) carrying the 6xHis tag. The hVDAC3 coding sequence was afterwards subcloned *in frame* to the Yellow Fluorescent Protein (YFP) in pEYFP-C3 vector [23]. This YFP-6His-hVDAC3 sequence was subsequently subcloned NheI/NotI in pEFIRES-P vector under the control of the strong human elongation factor 1a promoter [24]. The amino acid cleavage site ENLYFQG, target of TEV (Tobacco Etch Virus) protease, was next introduced between the YFP and the 6xHis sequences of the pEFIRES-YFP-6His-hVDAC3 construct by using the QuikChange XL Site-Directed Mutagenesis kit (Stratagene). The mutagenized final construct was named pEFIRES-YFP-TEV-6His-hVDAC3 (see Figure 1 for a detailed representation). Primers used in the site-directed mutagenesis were 5'-ATC TCG AGC TCA AGG AGA ATC TTT ACT TTC AAG GTC TTC CAC GCG TGC A-3' (forward primer) and 5'-TCG ACG CGT GGA AGA CCT TGA AAG TAA AGA TTC TCC TTG AGC TCG AGA T-3' (reverse primer). All constructs were verified by sequencing both strands.

2.2. Cell culture and generation of a stable cell line expressing the YFP-TEV-6His-hVDAC3 construct.

HeLa cells were cultured in Dulbecco's modified Eagle's medium supplemented with 10% fetal bovine serum, at 37°C in a humidified 5% CO₂ incubator. 2 x 10⁶ cells were plated in 90 mm culture plates and allowed to grow overnight. Next day cells were transfected with pEFIRES-YFP-TEV-6His-hVDAC3 DNA (100 µg/plate) using Lipofectamine 2000 (Invitrogen). Transfected cells were subjected to drug selection with decreasing concentration (from 5 to 1 µg/ml) of puromycin (Invitrogen) and replated at low density. Single colonies were isolated after three weeks. Several puromycin-resistant and fluorescent cell clones were established and the expression of YFP-TEV-6His-hVDAC3 verified by immunoblotting. The HeLa cell clone 1A4 was chosen for further experiments.

2.3 Quantitative RT-PCR amplification

Total cellular RNA was isolated from 1 x 10⁶ cells of the HeLa 1A4 stable clone. RNA concentration was evaluated using Quant-iT RNA Assay Kit with a Qubit fluorometer (Invitrogen). The first strand of cDNA was synthesized from 2 µg of total RNA using SuperScript II Reverse Transcriptase (Invitrogen). To quantify tagged-VDAC3 and wt-VDAC3 transcript levels in HeLa 1A4 cell, real-time amplification was performed in a Mastercycler EP Realplex (Eppendorf). The reaction mixture contained 1 µl of total cDNA and 0.4 µM of gene specific pairs of primers ((RTFw 867 VDAC3 (5'-CTGATTGGACTGGGTATATACT-3') and RTRev 92 GFP (5'-GACACGCTGAACCTTGTGGC-3') or RTFw 219 VDAC3 (5'-ACGGGATTGTTTTAGTGTTG-3') and RTRev 370 VDAC3 (5'-CTCCAGTTCAAATCCCAAGC-3')). The Real Master Mix SYBR ROX-2.5 (5 PRIME) was used. PCR program included one denaturing cycle at 95 °C for 2 min; 40 cycles 95 °C for 15 s, 53 °C for 15 s, 68 °C for 20 s. To calculate the copy number of the target genes in the samples, the standard curve method was used with as template human VDAC3 amplicon.

2.4. Cell lysis and Western blot analysis

The HeLa cell clone 1A4 was grown to 80% confluency (2 x 10⁷ cells) in a 75 cm² flask. Cells were detached with 2 mM EDTA/PBS for 5 minutes at 37°C, harvested, washed twice in ice-cold PBS and recovered by short centrifugation at 5.000 g, 4°C. Cells were then lysed in 1 ml of ice-cold lysis buffer LB (1% (v/v) Triton X-100, 10 mM NaCl, 10 mM Tris-HCl, pH 7.5, 1,5 mM MgCl₂, 1x Complete Protease EDTA-free inhibitor cocktail (Roche)). Cell lysates were cleared by centrifugation for 30 min at 12.000 g, 4°C. 50 µg protein were resolved on 10% SDS-PAGE and

transferred to a PVDF membrane (Millipore). The tagged VDAC3 protein in HeLa cell clone 1A4 was immunostained either with a polyclonal anti-GFP antibody (1:1000) (Rockland) or with an anti-RGS-His antibody (1:1000) (Qiagen); secondary anti-goat (used 1:15.000 in W. Blot) was from Santa Cruz and anti-mouse (used 1:15.000 in W. Blot) was from Amersham. Proteins were detected by using the enhanced chemiluminescence (ECL) system (Amersham Biosciences) and visualized by autoradiography.

2.5. Immunofluorescence assays

1A4 HeLa cells were seeded onto 6-well plates containing 12-mm-coverslips. After 48 h seeded cells were fixed in 4% paraformaldehyde for 20 min r.t., permeabilised in 0.5% Triton X-100 and incubated with 3% BSA to block unspecific binding. Cells were stained for YFP-6His-hVDAC3 with 1:100 anti-GFP or 1:100 anti-His (Santa Cruz), followed by secondary antibody conjugated with 1:300 Alexafluor-680 (Molecular Probes). Images were acquired a Leica TCS SL inverted laser scanning confocal microscope.

2.6. Live cell imaging

1A4 HeLa cells were seeded onto WILLCO 35 mm, thin glass-bottom-dishes (Intracel) and incubated overnight in D-MEM (minus phenol red) containing 10% fetal calf serum at 37°C in 5% CO₂. After 24 hr, cells were imaged at 37°C and 5% CO₂ within an open chamber system (Solent Scientific). Images were acquired using a DeltaVision microscope system (Applied Precision), consisting of an inverted microscope (Olympus IX70) with a 1.40 NA 60 X objective and Photometric CH300 CCD camera. 10 x 1 µm sections for YFP were taken at 15 min intervals over a 2 hr period. Images were deconvoluted using SoftWorx (Applied Precision).

2.7. Purification of native protein complexes interacting with tagged hVDAC3 protein

Figure 4 shows the whole purification strategy adopted in the work.

2.7.1. Purification of hVDAC3 interacting proteins by anti-GFP antibodies and magnetic IgG-beads.

1 x 10⁸ cells from HeLa cell clone 1A4 were grown to 80% confluency in 75 cm² flasks and lysed in ice with 0.75 ml/flask of cold LB. Lysed cells were scraped and incubated for 1 hour at 4°C, under gentle rotation. Cellular debris were removed from the lysate by centrifugation at 12.000 g for 30 min at 4°C and 2 ml (2 mg/ml) of supernatant was added to 4 µg of monoclonal anti-GFP (Roche). The lysate was rotated for 2 hours at 4°C. 750 µl of Dynabeads M-280 Sheep anti-Mouse IgG (Dyna) were washed three times with 5 ml ice-cold PBS supplemented with 0.1% BSA. The recovered beads were resuspend in 750 µl of LB and added to the lysate. The lysate was then

incubated with gentle rotation (400 rpm) overnight, at 4°C. After the incubation, the beads were recovered and washed three times with 750 µl of 1x AcTEV buffer (Invitrogen).

2.7.2. Cleavage with TEV protease.

Cleavage with AcTEV protease (Invitrogen) cut off the YFP and its interacting proteins from hVDAC3. TEV protease action was assayed, on the sample immunoprecipitated in the first step of purification, in 400 µl reactions at different TEV concentrations (2U/ or 20U/mg of total protein) and different time (2, 6 hours or overnight.). The best results were obtained by using 20U/mg total protein in an overnight reaction.

2.7.3. Purification of hVDAC3 interacting proteins by Ni-NTA magnetic agarose beads.

After TEV proteolysis, beads were collected and separated from the supernatant containing His-hVDAC3 and specific interacting partners. This sample underwent a next step of purification. 200 µl of Ni-NTA magnetic agarose beads (Qiagen) were washed twice in Ni-NTA wash buffer (50 mM NaH₂PO₄, 300 mM NaCl, 20 mM imidazole, 0.05% Tween 20, pH 8.0), resuspended in an equal volume of the same buffer and then added to the supernatant from TEV digestion. This sample was incubated under gentle rotated overnight, at 4°C. The beads were collected by a magnetic separator, washed three times in Ni-NTA wash buffer and at the end interacting proteins were detached by heating at 95°C in 200 µl SDS-sample buffer.

After each purification step, small aliquots of samples captured from beads and present in supernatant were removed and the cleavage product was monitored by Western-Blot.

2.8. Immunoprecipitation of PDI and PHB.

Protein disulfide isomerase (PDI) or prohibitin (PHB) were immunoprecipitated from 200 µl of lysate of 1A4 stable clone or HeLa cells as a control, by using 0.4 µg of monoclonal antibodies anti-PDI (Abcam) or anti-PHB (Santa Cruz), respectively. Any interaction of PDI or PHB with tagged or native VDAC3 was then assayed by capturing the immunocomplexes with 75 µl of IgG-coated magnetic beads. Immunoprecipitates were eluted with 20 µl of SDS sample buffer. 10 µl were separated in 12% SDS-PAGE and then blotted onto PVDF membranes. Western blots were probed with a 1:500 polyclonal anti-VDAC3 (Abcam) or a 1:2000 polyclonal anti-GFP (Rockland).

2.9. Two-Dimensional Gel Electrophoresis (2-DE)

The first dimension was run in a IEF-Protean apparatus (Bio-Rad), using IPG immobilized strip. 200 µl of Sample Rehydration Buffer (6 M urea, 2 M thiourea, 4% CHAPS, 20 mM DTT, 0.2%

ampholine (BioRad), 0.002% bromophenol blue) were added to 75 μ l of sample from the second purification step. The sample was actively rehydrated for 16 h. The conditions of IEF were: 15 minutes at 250 V (step 1); a voltage ramp of 2 h until 4000 V (step 2); a voltage ramp of 20 h until 20000 V (step 3); a constant voltage of 500V until the run end (step 4). Precast Bis-TrisHCl 4-12% gel (Invitrogen) and MOPS Running buffer (50 mM MOPS, 50 mM Tris Base, 0.1% SDS, 1 mM EDTA, pH 7.7) were used for the second dimension. Gels were revealed using Coomassie Blue staining.

2.10. Mass spectrometry analysis and protein identification

Protein spots were excised from gel and cut into 1 mm cubes. These were then subjected to in-gel digestion, using a ProGest Investigator in-gel digestion robot (Genomic Solutions, Ann Arbor, MI) using standard protocols [25]. Briefly the gel cubes were destained by washing with acetonitrile and subjected to reduction and alkylation before digestion with trypsin at 37°C. The peptides were extracted with 10% formic acid and concentrated down to 20 μ L using a SpeedVac (ThermoSavant). They were then separated using an UltiMate nanoLC (LC Packings, Amsterdam) equipped with a PepMap C18 trap & column, using a 60 min elution profile, with a gradient of increasing acetonitrile, containing 0.1 % formic acid, to elute the peptides (5-35% acetonitrile in 18 min, 35-50% in a further 7 min, followed by 95% acetonitrile to clean the column, before reequilibration to 5% acetonitrile). The eluent was sprayed into a Q-Star XL tandem mass spectrometer (Applied Biosystems, Foster City, CA) and analysed in Information Dependent Acquisition (IDA) mode, performing 1 sec of MS followed by 3 sec MSMS analyses of the 2 most intense peaks seen by MS. These masses are then excluded from analysis for the next 60 sec. MS/MS data for doubly and triply charged precursor ions was converted to centroid data, without smoothing, using the Analyst QS1.1 mascot.dll data import filter with default settings. The MS/MS data file generated was analysed using the Mascot 2.1 search engine (Matrix Science, London, UK) against UniProt with no species restriction. Data was searched with tolerances of 0.2 Da for the precursor and fragment ions, trypsin as the cleavage enzyme, one missed cleavage, carbamidomethyl modification of cysteines as a fixed modification and methionine oxidation selected as a variable modification. The Mascot search results were accepted if a protein hit included at least one peptide with a score above the homology threshold.

Organelle association for each identified protein was determined from GO annotation. The "Core Analysis' function included in IPA (Ingenuity System Inc, USA, www.ingenuity.com) was used to interpret the our data in the context of biological processes, disease pathways and cellular networks. Networks were customised starting from our protein list and comparing with molecular interactions

present in the Ingenuity Knowledge Database. For our network analysis we have chosen to include direct and indirect interaction and we customized to 35 nodes per network.

3. RESULTS

3.1 Generation of a stable mammalian cell line expressing a LAP-tagged hVDAC3 protein.

The N-terminal of the human VDAC3 coding sequence was fused with a distal YFP sequence and a proximal 6xHis-tag, separated by a proteolytic site specifically recognized by TEV protease (Fig. 1). This construct was cloned in pEFIRES-P, containing the human polypeptide chain elongation factor 1a (pEF-1a) promoter and an internal ribosome entry site (IRES). This vector directly links the expression of the gene of interest with the puromycin resistance gene, the next step for selection of stable clones. The YFP-TEV-6His-hVDAC3-pEFIRES-P plasmid was cloned and expressed in HeLa cells. We obtained several HeLa clones stably expressing our tagged hVDAC3 protein. The HeLa 1A4 cell clone expressed the tagged hVDAC3 at the same level as the endogenous hVDAC3 protein (Fig. S1) and was chosen for further live-cell imaging and purification of the cellular interactome of tagged hVDAC3. The selection of a stably expressing cellular clone was pursued to keep an homogenous and constant amount of bait protein in the cell. The expression of tagged hVDAC3 in the HeLa 1A4 cell clone was verified by Western Blot using antibodies against the tags (Fig. 2). Moreover, we have also checked transcription with RT-PCR: tagged VDAC3 was shown to be expressed in 1A4 HeLa cell clone (Fig. S1). In the same HeLa 1A4 cell, the correct localization to mitochondria could be established by indirect immunofluorescence assay (Fig. 3). The presence of the tag was not dependent on time: time course experiments show that YFP fluorescence is constantly expressed in the 1A4 HeLa cell clone (Fig. S2).

3.2 Purification of protein natively interacting with tagged hVDAC3 protein.

In our application of LAP-tag technology, we used two different steps of purification in native condition. Figure 4 shows the whole purification strategy adopted in the work. In the first purification step, the immunoprecipitation of the protein complex interacting with tagged hVDAC3 was performed upon incubation of cellular lysates of 1A4 HeLa cell clone with an anti-GFP antibody and next by the interaction and collection of the immuno-complex with IgG-coated magnetic beads (Fig. 4).

The mixture of hVDAC3 and interacting proteins was then digested with TEV protease at different times and concentrations. Western blots of beads-linked proteins or supernatant proteins performed with anti-His or anti-GFP antibodies showed that the optimal condition was found to be 20 U of

protease/mg of total protein and an overnight reaction (Fig. 5). After cleavage with the TEV protease, the hVDAC3 His-tag became exposed, while the YFP-interacting proteins were released, together with magnetic beads and any interacting background proteins. Proteins interacting with the 6xHis-tag-hVDAC3 were further pulled down using the exposed tag as the bait for nickel-nitrilotriacetic acid-coated magnetic beads. Proteins pulled-down by the magnetic beads were recovered in SDS-sample buffer (SSB).

3.3 Analysis of the purified hVDAC3 interactome and protein identification

Proteins isolated from the second LAP-tag purification step were resolved on a two dimensional gel electrophoresis (2D-GE) and 43 spots were detected with Blue Coomassie stain (Fig. S3). The 2D-GE was repeated three times; an example is shown in Figure S3A. It must be taken into account that the yield of purified protein is very low, even though we used a stable cell clone. As a control, we applied the same LAP-tag procedure to HeLa cells transfected with the empty pEFIRES-P vector, under the same condition used to purify the VDAC3 interacting proteins and only few spots were detected (Fig. S3C). In another preliminary experiment we have compared the protein pattern obtained with a construct similar, but carrying VDAC2, in 2D-GE. The pattern of spots was clearly different (not shown). The visible spots were excised from the gel (Fig. S3B), trypsinized and then analyzed by mass spectrometry as described in the methods. Peak profiling used the Mascot search engine whereby mass spectra were matched against the NCBI non-redundant database. The protein score was very high for the most of excised spots, and the sequence coverage was also very significant (Table 1).

Co-immunoprecipitation of the same representative proteins was used as a methodological validation of our experiment. Figure 6 shows the presence of the VDAC3-YFP construct in samples immunoprecipitated with anti-prohibitin (PHB) or anti-protein disulfide isomerase (PDI) antibodies. This experiment was performed after the first LAP-tag purification step, due to the paucity of material available in the procedure. The same experiment, performed with a generic antibody (IgG), does not show any immunoprecipitate. In a lysate from HeLa cell not transfected with our plasmid only the faint band corresponding to VDAC3 was co-immunoprecipitated by the antibodies (Fig. 6).

3.4 Proteins interacting with VDAC3.

The list of proteins identified in excised spots by Mass spectrometry is reported in Table 1. The table shows the spot number (as noted in Figure S3B), the estimated Mr and pI, information on the identified protein. The coverage is usually pretty high, in the order of 50%, a direct validation of identification itself. The protein symbol is reported in the last column and it has been utilized in a

general scheme of VDAC3 interactors protein. The list has been provided to the Ingenuity Software suite for an automatic analysis of the interactors and their relationships.

Figure 7 reports the bioinformatic analysis of the list of VDAC3 interactors. Using Gene Ontology (GO) annotation a graphical view of the endocellular origin of the detected protein is reported in Figure 7A. About half of them are cytosolic proteins, a not surprising data, since VDAC3 is located at the interface with the cytosol. Approximately 15% aliquots of the overall proteins found as hVDAC3 interactors are components of three other relevant cellular subcompartments, namely mitochondria, endoplasmic reticulum and cytoskeleton (Fig. 7A). To unravel information embedded in the list of identified proteins, it was submitted to the Ingenuity Pathway Analysis (IPA) software. Figure 7B shows the most relevant functional pathways for identified proteins: the processes that obtained the highest score, by far highest than the threshold, were pathway for post-translational modification and folding, a somehow unexpected finding, followed by apoptosis, energy production, biochemistry of small molecules and cellular growth and morphology, a set of processes that are more intuitively related to VDAC proteins. The same kind of analysis, aimed to discovery of pathological processes (Fig. 7C), reveals a large spectra of pathological area. The most relevant is cancer but, interestingly, reproductive system diseases have almost the same score: it is known that VDAC3 is highly expressed in testis [26] and has been found to be abundant in spermatozoa [21]. In general, the disorders shown in Figure 7C have yet to be attributed to the activity of VDAC3 and targeted analysis of the proteins in these pathways could lead to a new appreciation for a VDAC3-based mechanism for these disorders.

The IPA software was also used to graphically represent the main networks found within the list of hVDAC3 interactors. Figure 8A shows the network mainly associated with cell morphology, cellular assembly and organization, where 23 proteins are found with a score of 55, while Figure 8B is the second high-score network found with IPA, with 19 proteins and a score of 43, associated mainly with post-translational modification and protein folding.

DISCUSSION

The difficulties implied in interactomic analysis of membrane embedded proteins are demonstrated by the paucity of reports concerning this topic existing in the literature. There are indeed numerous experimental tools to identify the interaction network of soluble proteins, but strategies for the identification of membrane protein interactomes remain limited. Innovative and highly imaginative methods need to be designed to climb this difficult task. For example, recently a new approach has

been introduced by Gochale et al: they used covalent chemical stabilizers of protein-protein interactions combined with magnetic bead immuno-affinity chromatography, quantitative SILAC mass-spectrometry and in silico network construction [27]. VDAC1 and 2 are known to interact with several proteins like Bcl2, Bak, Hexokinases, Tubulin, gelsolin and mutant SOD1 (see [2]). Possibly more proteins are involved in interactions. The reason for these claims is because VDAC isoforms in the outer mitochondrial membrane are in a crucial position as the interface between the mitochondrial borders/metabolism and the rest-of-the-cell pathways and structures. VDACS are suspected to take part in receptors or docking complexes on the mitochondria surface. It is thus an urgent task to know the number and the nature of the proteins that interact stably enough with these proteins.

There is a single work in the literature reporting a systematic approach to the interactome of VDAC1, the most abundant isoform [28]. The group of Zizi immobilized VDAC1-containing proteoliposomes on a chip surface. Using microfluidics, they screened a liver cDNA phage display library by a surface plasmon resonance device. In this way, they obtained a list of VDAC1 interactors. The aim was to maximize the likelihood of ligands to the target native folds and avoid selecting interfering proteins by incorporation of VDAC1 into liposomes. This work was remarkable, even though the experimental conditions are not comparable to those existing in the cell. In addition a specific technological expertise is requested for this kind of work.

Our approach aimed to detect the interactions in a more physiological cellular context. In our system, VDAC3 with two added tags was expressed in cultured cells. It could interact with proteins in the cell in its transmembrane localization, confirmed by confocal microscopy. The enrichment of the tagged protein was obtained by establishing a cell clone stably expressing the protein. The second step, after the proteolytic cleavage, had the purpose to drastically reducing the interaction with proteins aspecifically adsorbed to the complex. The promising consequence of the LAP-tag method is indeed the strong reduction of unspecifically interacting, or aggregates, proteins to the isolated complex [29]. Thus, this purification procedure resolves the very common and unwanted side-result of more traditional techniques ranging from simple immunoprecipitation to the double-hybrid yeast strategy. This means that our list of VDAC3 interacting proteins is more tenable than any other information obtained before and can thus be of the highest relevance to guide further investigation into the role of this rather mysterious protein.

The proteomic analysis resulted in the list of putative interacting proteins (Table 1). The most stimulating goal in this kind of work is to find a cellular rationale to the components of the interactomic complex. We have largely used bioinformatic tools to organize the various members of the list and to data mining their relative meaning. An effort to produce a panoramic view of

VDAC3 interaction and functional connections is given in Figure 9, where the proteins from Table 1 are reported with the same symbol names and are colour and space coded in specific cellular subcompartment or representative cellular processes. Proteins are grouped outside the mitochondrion or in it on the basis of the most relevant cellular process. In some cases, the same protein can be found twice, depending on its presence in more pathways. The coloured boxes correspond to large assemblies related to a common cellular process and are sometime located in definite subcellular compartments.

Some proteins from the mitochondrion were detected in our study: carbamoylphosphate synthetase I, for example; prohibitin, a protein that plays a role in the organization of the cristae and is thus involved in contacts with the outer membrane; and the subunit d of the ATP synthase, a non-integral membrane component of the membrane pore domain required for proper assembly of the membrane sector. Also Roman et al detected ATPase subunits 6 and epsilon [28] among VDAC1 interactors.

Therefore, the highest number of identified proteins were cytoplasmic proteins such as components of Hsp family, some proteins belonging to 14-3-3 family (implicated in the regulation of a large spectrum of both general and specialized signaling pathways) or some enzymes as PRDXs or GSTO-1 (enzymes involved in the protection of cells against oxidative stress), and some proteins able to act as transport proteins as PI-6 or VCP (that transfers membranes from the ER to the Golgi apparatus via specific transition vesicles).

One of the most represented compartment (Tab. 1) is the ER. Communication between endoplasmic reticulum and mitochondria is achieved by mitochondria-associate membranes (MAM), regions required for many key cellular events [30]. Interestingly Grp78, HspA9 and calreticulin (in box C, Fig. 9) and the same VDAC isoforms are markers of MAM [31]. The endoplasmic reticulum faces accumulation of mis-folded or unfolded proteins by the ER-associated degradation pathway (ERAD) and through chaperones, oxidases e thiol isomerases (like PDI or Erp5, box C, Fig. 9). The process precedes protein traslocation to proteasome/Ub system, in cytosol (ubiquitination and/or proteasome have an ATP-dependent activity) [32]. In addition proteasome/Ub system has been reported to work as a quality control of mitochondrial proteostasis: degradation of specific OMM proteins and of the same VDAC1 is considered a prerequisite of mitophagy [33-34]. Also prohibitin (Fig. 9, in mitochondrion), whose interaction with VDAC3 has been validated here, looks to be involved in IMM protein turnover [35]. VCP is a member of the ERAD pathway [36-37] (in boxes C and D, Fig. 9) and is involved in the “extraction” of protein from the OMM and other membranes to be directed to ubiquitination and degradation through ER, with or without stress conditions [33]. It is important to remember that VCP mutants have been correlated to the onset of some type of

myopathies, of frontotemporal dementia and of Alzheimer, Parkinsons or Amyotrophic Lateral Sclerosis, all pathologies where VDAC is certainly involved.

The mammalian unfolded protein response (UPR) involves 2 main mechanisms able to counteract misfolded proteins: up-regulating chaperons and proteolytic degradation involving ubiquitin-proteasome and autophagy-lysosome system [38]. Upon failure of these systems, abnormal proteins form aggregates that can be transported into aggresome, centrosome-associated structures, where they are degraded [39]. In the box D of Fig. 9 are present some proteins linked to aggresome, as YWHAQ, KCIP1 or SFN.

Therefore, the connection between VDAC3 and the processes related to organization, maturation and recycling of proteins cannot be a simple coincidence since members of the pathways related to translation and ribosomal control (Box E), proteasomal components (Box D), chaperons (Box D), ER and Golgi have been localized (Fig. 9). Interestingly also in the interactor list reported by Roman et al for VDAC1, proteasome and ribosomal proteins have been found, indicating that a link between the mitochondrion surface (OMM) and the protein synthesis is more direct than expected. Less surprising is the presence of several cytoskeletal and centrosomal proteins correlated to VDAC3 (box F and cytoskeleton, in Fig. 9). Various tubulins and some cytokeratins have been detected among the spots. It is known that tubulin is a modulator of VDAC1 and VDAC2 channel activity [40]. Recently it has been found that VDAC 3 is less sensitive than the other isoforms to tubulin interaction, reinforcing the hypothesis that VDAC3 is mainly involved in organizational processes of subcellular structures [19-21]. Serpin B6 is a serine protease inhibitor expressed at centrosome and cytosol level. Control experiments demonstrated that cytoskeletal proteins are not the result of trivial contamination. VCP is also in the cytosol and could act towards VDAC3, maybe after some VDAC3 specific residue's modification, "extracting" a modified (inactivated?) version of this protein, addressing it toward microtubules through cytoplasmic granules' traffic [41] and enriching near the centrosome. VDAC3 has been detected at the centriole and a regulatory role in ciliogenesis has been proposed [20, 42]. A similar traffic can explain the presence of VDAC3 in the ODF in the sperm tail [21].

Some proteins involved in maintaining the redox status are also detected as VDAC3 interactors: for example, isoforms of protein disulfide isomerases, peroxiredoxins, glutathione transferases. The interaction of VDAC3 and Glutathione S-transferase Kinase 1 (GSTK-1) has been found [43]. This raises the intriguing possibility that VDAC3, with its large number of cysteines, can be involved in a redox signaling pathway and in protection against oxidative injury [14, 44].

In addition, many of the identified proteins are also involved in the response to virus. It has been reported that HBx protein, encoded by Hepatitis B Virus (HBV), directly interacts with VDAC3

[45], altering the mitochondrial transmembrane potential. So, it is possible that mitochondrial dysfunction related to other viral infections is due to recruitment to the mitochondria of some proteins identified in this study.

GRP75/HspA9/mtHSP70 is a stress proteins interacting with VDAC1 [46]. Other similar proteins have been identified in our study, underlying that VDAC3 is probably involved in transport or processing of proteins generated under stress conditions in different cell compartments.

We identified significantly overrepresented disease pathways with IPA software. Cancer, organismal injury and abnormalities, respiratory or reproductive system disease, renal or dermatological disease, and neurological disease are the principal pathways recognized. Many of these pathways are related to tissue with ciliate cells. Furthermore the only uncharacterized protein identified (Uniprot ID Q9BU08, in Table 1) with this study belongs to TCP1 chaperone family. These chaperones can be act as part of the BBS/CCT complex that may play a role in the assembly of BBSome, a complex involved in ciliogenesis regulating transports vesicles to the cilia.

The main conclusion is that VDAC3 is apparently associated to patterns involved in the organization of protein complexes, in different subcellular compartments. In addition VDAC3 isoform could play a pivotal role in the regulation of the traffic of misfolded or non-folded proteins evoked from different stimuli, with the likely aim of addressing to degradation misfolded mitochondrial proteins, and rescuing the organelle by the damages. This is supported by the Parkin recruitment to defective mitochondria through VDAC1, 2 and 3 to promote mitochondrial autophagy [47]. K.O. mouse for VDAC3 gene are male sterile due to immotile sperms for defective axoneme and disassembled mitochondria in epididymal sperm [19, 21].

VDAC is a family of proteins whose primary role is to channel through the mitochondrial outer membrane hydrophilic metabolites and molecules. This strategic localization is raising many new questions that are essentially linked to the possibility that VDACS can be a docking site for other proteins on both sides of the membrane. These candidate proteins could have an influence upon the channel activity or can just utilize VDAC as a dock on the outer membrane. A further complication is given by the presence in the MOM of three different isoforms, whose specific and individual roles are the object of much speculation. VDAC3 is the most intriguing because the least known: it has not been properly characterized from a functional point of view. It is the isoform showing to have the largest number of interactions with cytoskeletal proteins, making it a candidate for a role as a contact point. In addition, VDAC3 has been found, or it is at least suspected, to be in other subcellular compartments in addition to mitochondria [20, 42].

The work presented here sheds some preliminary light on the potential network of interactors involving VDAC3. We have proposed and applied a strategy for a single membrane protein, VDAC3. We are now working to apply a similar strategy to the other VDAC isoforms and to other small transmembrane protein like the metabolite carriers.

Acknowledgments

This work has been produced in the frame of the Italian initiative for the Human Proteomic Project [48]. The authors acknowledge the financial support by PRIN 2010CSJX4F. A.M. acknowledges the financial support by ARISLA. The authors thank the St Andrews Mass Spectrometry Facility, which is funded by the Wellcome Trust.

References

1. Colombini, M. (1980) Structure and mode of action of a voltage dependent anion-selective channel (VDAC) located in the outer mitochondrial membrane. *Ann. N.Y. Acad. Sci.* 341, 552–563.
2. Shoshan-Barmatz V., De Pinto V., Zweckstetter M., Raviv Z., Keinan N. (2010) VDAC, a multi-functional mitochondrial protein regulating cell life and death. *Mol. Aspects Med.* 31, 227-285.
3. Rostovtseva T. and Colombini M. (1997) VDAC channels mediate and gate the flow of ATP: implications for the regulation of mitochondrial function. *Biophys J.* 72, 1954-62.
4. Kroemer G., Galluzzi L. and Brenner C. (2007) Mitochondrial Membrane Permeabilization in Cell Death. *Physiol. Rev.* 87, 99-163.
5. Tomasello F., Messina A., Lartigue L., Schembri L., Medina C., Reina S., et al (2009) Outer membrane VDAC1 controls permeability transition of the inner mitochondrial membrane in cellulo during stress-induced apoptosis. *Cell Res.* 19, 1363-76.
6. De Stefani D., Bononi A., Romagnoli A., Messina A., De Pinto V., Pinton P., and Rizzuto R. (2012) VDAC1 selectively transfers apoptotic Ca(2+) signals to mitochondria. *Cell Death Differ.* 19, 267-73.
7. Shoshan-Barmatz V. and Mizrahi D. (2012) VDAC1: from structure to cancer therapy. *Front. Oncol.* 2, 164
8. Huizing M., Ruitenbeek W., Thinnen F., and De Pinto V. (1994) Deficiency of the Voltage-Dependent Anion Channel (VDAC): a novel cause of mitochondrial myopathies. *The Lancet* 344, 762.
9. Hiller S., Garces R.G., Malia T.J., Orekhov V.Y., Colombini M. and Wagner G. (2008) Solution structure of the integral human membrane protein VDAC-1 in detergent micelles. *Science* 321, 1206-1210.
10. Bayrhuber M., Meins T., Habeck M., Becker S., Giller K. et al. (2008) Structure of the human voltage-dependent anion channel. *Proc. Natl. Acad. Sci. USA* 105, 15370-15375.
11. Ujwal R., Cascio D., Colletier J.P., Faham S., Zhang J. et al. (2008) The crystal structure of mouse VDAC1 at 2.3 angstrom resolution reveals mechanistic insights into metabolite gating. *Proc. Natl. Acad. Sci. USA* 105, 17742-17747.
12. De Pinto V., Reina S., Guarino F., and Messina A. (2008) The structure of Voltage-Dependent Anion selective Channel: state of the art. *J. Bioenerg. Biomembr.* 40, 139-147.
13. Tomasello F.M., Guarino F., Messina A., Reina S., De Pinto V. (2013) The Voltage-Dependent Anion selective Channel 1 (VDAC1) topography in the mitochondrial outer membrane as detected in intact cell. *Plos One*, 8, e81522.
14. De Pinto V., Guarino F., Guarnera A., Messina A., Reina S., Tomasello F.M., Palermo V., Mazzoni C. (2010) Characterization of human VDAC isoforms: a peculiar function for VDAC3?, *Biochim. Biophys. Acta* 1797, 1268-1275.
15. Messina A., Reina S., Guarino F., and De Pinto V. (2012) VDAC isoforms in mammals. *Biochim. Biophys. Acta* 181, 1466-76.
16. Xu X., Decker W., Sampson M.J., Craigen W.J. and Colombini, M. (1999) Mouse VDAC isoforms expressed in yeast: channel properties and their roles in mitochondrial outer membrane permeability. *J. Membr. Biol.* 170, 89–102.
17. Reina S., Palermo V., Guarino F., Messina A., Mazzoni C. et al. (2010) Swapping of the N-terminus of VDAC1 with VDAC3 restores full activity of the channel and confers anti-aging features to the cell. *FEBS Lett.* 584, 2837-2844.
18. Reina S., Magri A., Lolicato M., Guarino F., Impellizzeri A., Maier E., Benz R., Ceccarelli M., De Pinto V. and Messina A. (2013) Deletion of β -strands 9 and 10 converts VDAC1 voltage-dependence in an asymmetrical process. *Biochim. Biophys. Acta* 1827, 793-805.
19. Sampson M.J., Decker W.K., Beaudet A.L., Ruitenbeek W., Armstrong D., Hicks M.J. and Craigen W.J. (2001) Immotile sperm and infertility in mice lacking mitochondrial voltage-dependent anion channel type 3. *J. Biol. Chem.* 276, 39206–39212.
20. Majumder S., Slabodnick M., Pike A., Marquardt J. and Fisk H.A. (2012) VDAC3 regulates centriole

- assembly by targeting Mps1 to centrosomes. *Cell Cycle* 11, 3666-3678.
21. Hinsch K.D, De Pinto V., Aires V.A, Schneider X, Messina A. and Hinsch E. (2004) Voltage-dependent anion selective channels VDAC2 and VDAC3 are abundant proteins in bovine outer dense fibers, a cytoskeletal component of the sperm flagellum. *J. Biol. Chem.* 279, 15281-15288.
22. Rigaut G., Shevchenko A., Rutz B., Wilm M., Mann M. and Séraphin B. (1999) A generic protein purification method for protein complex characterization and proteome exploration. *Nat. Biotechnol.* 17, 1030-1032.
23. Rolls M.M., Stein P.A., Taylor S.S., Ha E., McKeon F and Rapoport T.A. (1999) A visual screen of a GFP-fusion library identifies a new type of nuclear envelope membrane protein. *J. Cell Biol.* 146, 29-42.
24. Hobbs S., Jitrapakdee S. and Wallace J.C. (1998) Development of a bicistronic vector driven by the human polypeptide chain elongation factor 1alpha promoter for creation of stable mammalian cell lines that express very high levels of recombinant proteins. *Biochem. Biophys. Res. Commun.* 252, 368-72.
25. Shevchenko A., Wilm M., Vorm O. and Mann M. (1996) Mass spectrometric sequencing of proteins silver-stained polyacrylamide gels. *Anal. Chem.* 68, 850-858.
26. Hinsch K.D., Asmarinah, Hinsch E., Konrad L. (2001) VDAC2 (porin-2) expression pattern and localization in the bovine testis. *Biochim Biophys Acta.* 1518, 29-33.
27. Gokhale A., Perez-Cornejo P., Duran C., Hartzell H.C. and Faundez V. (2012) A comprehensive strategy to identify stoichiometric membrane protein interactomes. *Cell Logist.* 2, 189-196.
28. Roman I., Figys J., Steurs G., Zizi M. (2006) Hunting interactomes of a membrane protein: obtaining the largest set of voltage-dependent anion channel-interacting protein epitopes. *Mol. Cell. Proteomics* 5, 1667-80.
29. Zanin E., Dumont J., Gassmann R., Cheeseman I., Maddox P., Bahmanyar S., Carvalho A., Niessen S., Yates III J.R. Oegema K, and Desai A. (2011) Affinity Purification of Protein Complexes in *C. elegans*. *Methods Cell Biol.* 106, 289–322.
30. Raturi A. and Simmen T. (2013) Where the endoplasmic reticulum and the mitochondrion tie the knot: the mitochondria-associated membrane (MAM). *Biochim. Biophys. Acta* 1833, 213-24.
31. Poston C.N., Krishnan S.C., Bazemore-Walker C.R. (2013) In-depth proteomic analysis of mammalian mitochondria-associated membranes (MAM). *J. Proteomics* 79, 219-30.
32. Heo J.M., Livnat-Levanon N., Taylor E.B., Jones K.T., Dephore N., et al. (2010) A stress-responsive system for mitochondrial protein degradation. *Mol. Cell.* 40, 465-480.
33. Karbowski M., Youle R.J. (2011) Regulating mitochondrial outer membrane proteins by ubiquitination and proteasomal degradation. *Curr. Opin. Cell Biol.* 23, 476-82.
34. Geisler S., Holmstrom K.M., Skujat D., Fiesel F.C., Rothfuss O.C., Kahle P.J., Springer W. (2010) PINK1/Parkin-mediated mitophagy is dependent on VDAC1 and p62/SQSTM1. *Nat. Cell Biol.* 12, 119-131.
35. Margineantu D.H., Emerson C.B., Diaz D., Hockenbery D.M. (2007) Hsp90 inhibition decreases mitochondrial protein turnover. *PLoS ONE* 2, e1066.
36. Olzmann J.A., Kopito R.R. and Christianson J.C. (2013) The Mammalian Endoplasmic Reticulum-Associated Degradation System. *Cold Spring Harb Perspect Biol* 5, a013185.
37. Xu S., Peng G., Wang Y., Fang S., Karbowski M. (2011) The AAA-ATPase p97 is essential for outer mitochondrial membrane protein turnover. *Mol. Biol. Cell.* 22, 291-300.
38. Bernales B., McDonald K.L. and Walter P. (2006) Autophagy counterbalances endoplasmic reticulum expansion during unfolded protein response *PloS Biol.* 4:e423.
39. Corboy M.J., Thomas P.J., Wigley W.C. (2005) Aggresome formation. *Methods Mol. Biol.* 301, 305-327.
40. Rostovtseva T.K., Bezrukov S.M. (2012) VDAC inhibition by tubulin and its physiological implications. *Biochim. Biophys. Acta* 1818, 1526-35.
41. Thomas M.G., Loschi M., Desbats M.A. and Boccaccio G.L (2011) RNA granules: the good, the bad and the ugly. *Cell Signal.* 23, 324-334.
42. Majumder S., Fisk H.A. (2013) VDAC3 and Mps1 negatively regulate ciliogenesis. *Cell Cycle* 12, 849-858.
43. Ewing R.M., Chu P., Elisma F., Li H., et al. (2007) Large-scale mapping of human protein-protein interactions by mass spectrometry. *Mol Syst Biol.* 3, 89.
44. Mailloux R.J., Jin X. and Willmore W.G. (2014) Redox regulation of mitochondrial function with

emphasis on cysteine oxidation reactions. *Redox Biol.* 2, 123-139.

45. Rahmani Z., Huh Kyung-Won, Lasher R. and Siddiqui A. (2000) Hepatitis B virus X protein colocalizes to mitochondria with a human voltage-dependent anion channel, HVDAC3, and alters its transmembrane potential. *J. Virol.* 74, 2840-2846.

46. Schwarzer C., Barnikol-Watanabe S., Thinnes F.P. and Hilschmann N. (2002) Voltage-dependent anion-selective channel (VDAC) interacts with the dynein light chain Tctex1 and the heat-shock protein PBP74. *Int. J. Biochem. Cell Biol.* 34, 1059-70.

47. Sun Y., Vashisht A.A., Tchiew J., Wohlschlegel J.A., Dreier L. Voltage-dependent anion channels (VDACs) recruit Parkin to defective mitochondria to promote mitochondrial autophagy. (2012) *J. Biol. Chem.* 287, 40652-60.

48. Urbani A., et al. (2013) The mitochondrial Italian Human Proteome Project initiative (mt-HPP). *Mol Biosyst.* 8, 1984-92.

49. Bellia F., Calabrese V., Guarino F., Cavallaro M., Cornelius C., De Pinto V., Rizzarelli E. (2009) Carnosinase levels in aging brain: redox state induction and cellular stress response. *Antioxid Redox Signal.* 11, 2759-75.

Figure Legends

Figure 1. The construct used in this work. The construct is based on pEFIRES-P. The yellow box shows the last coding triplet of the YFP; the green box is the TEV cleavage sequence; the purple box is the 6 x His tag. The whole sequence from YFP to VDAC3 (included) is in frame.

Figure 2. Western blot analysis of 1A4 HeLa cell lysates showing the expression of the construct YFP-TEV-6His-hVDAC3. Lysates of 1A4 cells were electrophoresed, blotted and immunostained with antibodies against the 6xHis tag (left panel) or the GFP (right panel). C-: negative control, lysate of HeLa cells; C+: positive control; S: cellular lysate from the stable clone 1A4. Positive controls were other proteins containing respectively a 6xHis tag (Carnosinase [49]) or the GFP itself. The Mr marker position is shown.

Figure 3. Immunostaining of the stable 1A4 HeLa cell clone. A: 1A4 cell were fixed and stained with DAPI (for nuclei, blue), antibodies against YFP (green) and antibodies against cytochrome c (red). The merged image obtained by confocal microscopy shows the co-localization in the mitochondrial network of YFP-TEV-6His-hVDAC3 and cytochrome c. B: close-up view of mitochondria in 1A4 HeLa cell first stained with Mitotracker Red (Invitrogen), then fixed and double stained with antibodies against GFP. The figure shows not only the co-localization but also the subtle difference between a protein in the outer membrane and the mitochondrial matrix.

Figure 4. Cartoon depicting the localization and affinity purification (LAP-tag) strategy used in this work. The LAP-tag strategy combines the advantages of generating a fluorescent protein fusion such as YFP with flexibility of the tandem affinity purification (TAP) tag.

Figure 5. Separation of YFP tag from the 6xHis-VDAC3. 1A4 HeLa cell lysates were incubated with TEV protease at different times. Next, beads coated with anti-GFP antibodies were magnetically separated from the supernatant. Western blots were performed upon protein associated with beads and the respective supernatant fraction. Both anti-6xHis or anti-GFP antibodies were used for staining. A: beads'pellet stained with antibodies anti-6xHis; B: supernatant stained with antibodies anti-6xHis; C: beads'pellet stained with antibodies anti-GFP; D: supernatant stained with antibodies anti-GFP. The Mr marker position is shown.

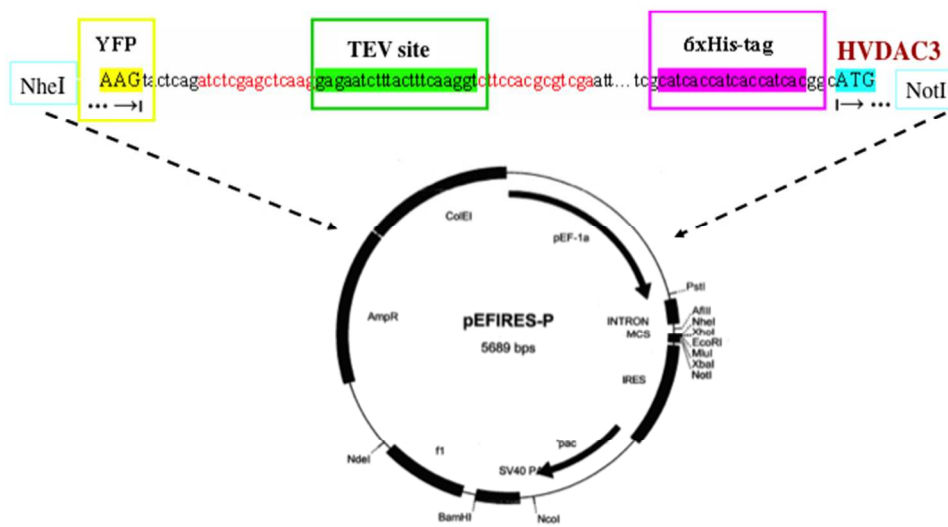
Figure 6. Co-immunoprecipitation of VDAC3 with Protein disulfide isomerase (PDI) and prohibitin (PHB). 1A4 HeLa cells were lysed and incubated with Ab anti-PDI (A) or anti-prohibitin (PHB) (B). The immunoprecipitated sample was solubilized with SDS-sample buffer, electrophoresed and immunodecorated with antibodies against VDAC3. HeLa indicates a control procedure performed upon not-transfected HeLa cells. PDI, PHB and IgG indicate the antibodies used to perform co-immunoprecipitation. V3-YFP is the migration of the fusion protein VDAC3-YFP; V3 is the migration of endogenous VDAC3. AbGFP are the same samples immunodecorated with anti-GFP Ab. AbPDI or AbPHB are the same samples immunodecorated respectively with anti-PDI or anti-PHB Abs.

Figure 7. Localization, biological functions and disease pathways of identified proteins. 61 proteins were identified in the interactome of VDAC3 from HeLa cells (Tab. 1). (A) Cellular localization for each protein was determined from GO annotation. Ingenuity Core Analysis was used to identify the most significant biological processes (B) and disease pathways (C).

Figure 8. The most significant biological functional networks identified by the Ingenuity Core Analysis software. (A) Network for cell morphology, cellular assembly and organization. 83% of all proteins in this network are proteins recognized in our work. This network got the highest score (55%). 23/35 proteins are present in Table 1 (PDI, TBP-1, KCIP-1, MSS1 and K17 are indicated in this network as P4HB, PSMC3, YWHAZ, PSMC2 and KRT17, respectively), and 6/35 correspond to protein families (i.e. cytokeratin or 14-3-3) or complexes (i.e. ATPase, 20s proteasome and PSMA) of which we found some components. **(B) Network for post-translational modifications, protein folding, cell compromise.** 72 % of all proteins in this network are proteins recognized in our work. This network got the second highest score (45%). 20/35 proteins are present in Table 1 (TUBB2C, Hip, HspA1A, Hsp90AB1, GRP75, ORP150, NPM, hTM5 and 37LRP are indicated in this network as TUBB4B, ST13, Hsp70, Hsp90, HspA9, HYOU1, NPM1, TPM3 and RPSA, respectively) and 2/35 correspond to protein complexes (i.e. 26s proteasome and HSP) of which we found some components. Colors: Fuchsia, peptidases; Red, complex/group; Light Blue, enzyme; Violet, transporter/ion channels; Grey, transcription regulator; Yellow, others. Continuous lines are direct relationships, dotted lines are indirect relationships; solid arrows represent known physical interactions. Ingenuity Core Analysis was used with default filters.

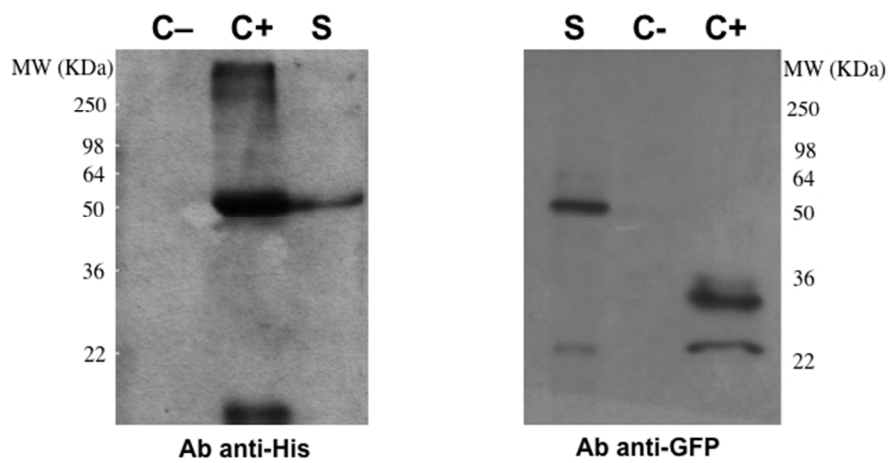
Figure 9. VDAC3 interactors in HeLa cells. Colored boxes show cellular compartments or protein groups with similar functions: **A**, enzymes or proteins with uncorrelated functions; **B**, proteins correlated to oxidative-stress; **C**, response to unfolded or misfolded proteins; **D**, proteasomal components and chaperons; **E**, proteins related to ribosome or to translational control; **F**, centrosomal proteins; **G**: chaperons, related or not to the aggresome; **ER**: Endoplasmic Reticulum; **Golgi**: Golgi Apparatus; **OMM**, outer mitochondrial membrane. The code for single proteins (circled) is the following: **blue**, response to stress; **dark-orange**, cell redox homeostasis; **dark-violet**, formation/rearrangement of disulfide bonds; **grey**, related to glycolysis; **yellow**, response to unfolded proteins or protein folding; **light-orange**, microtubules components; **brown**, ribosome biogenesis or RNA linking; **pink**, other functions. The inward colour blend indicates an ATP-binding site (i.e VCP). The outward colour blend indicates Ca^{2+} -binding (i.e. TCTP). The spotted line circle indicates a response to endoplasmic reticulum stress. The dotted line circles indicate a response to virus. The red line circles indicate chaperones. The black line circles indicate enzymes. The brown line circles indicate degradation of ubiquitinated proteins. Protein names written in blue indicate a link with disease. Circles drawn as in touch represent interacting proteins as found in Netpath, Hprd Database or in literature.

Figure 1, Messina et al



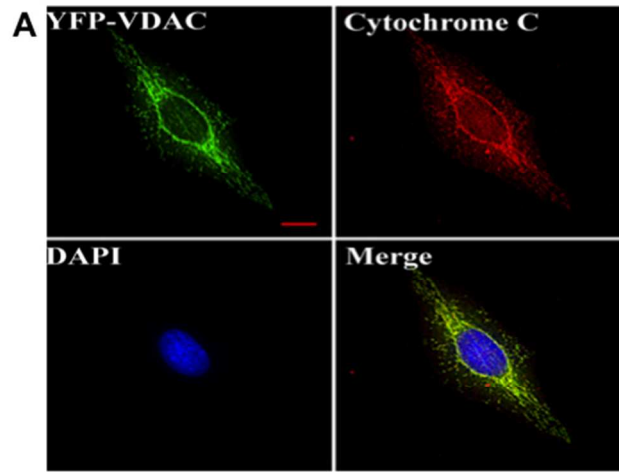
254x190mm (72 x 72 DPI)

Figure 2, Messina et al



254x190mm (72 x 72 DPI)

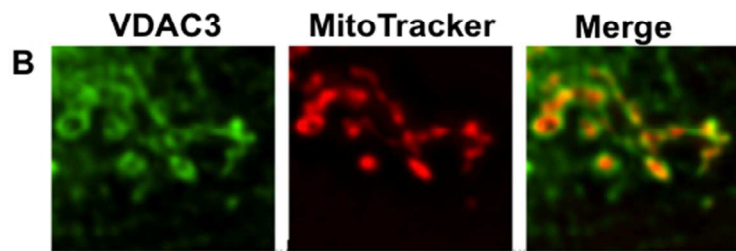
Figure 3A, Messina et al



3

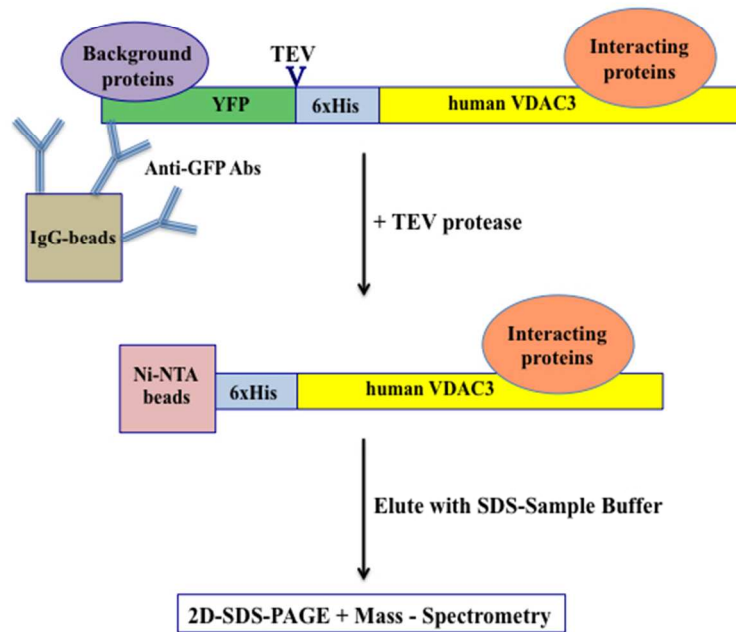
254x190mm (72 x 72 DPI)

Figure 3B, Messina et al



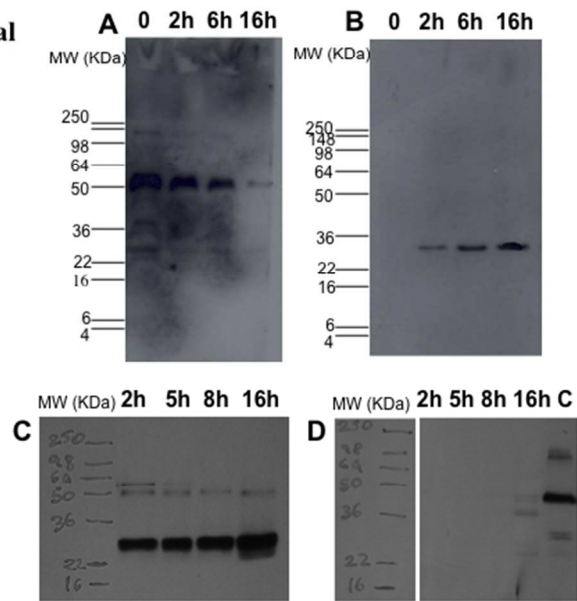
254x190mm (72 x 72 DPI)

Figure 4, Messina et al

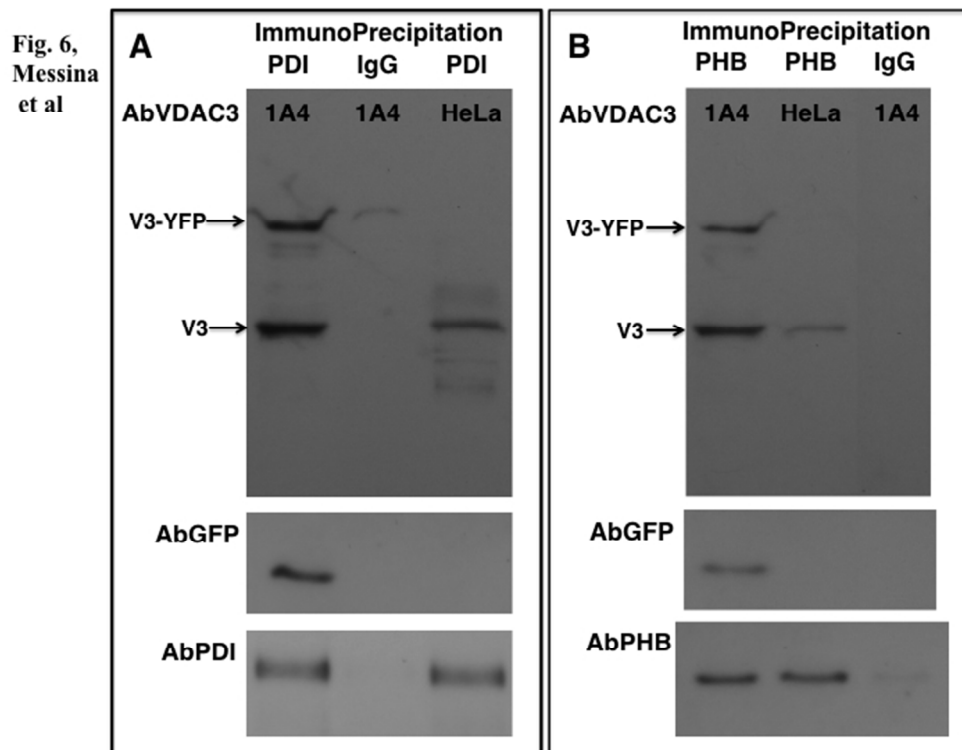


254x190mm (72 x 72 DPI)

Figure 5,
Messina et al

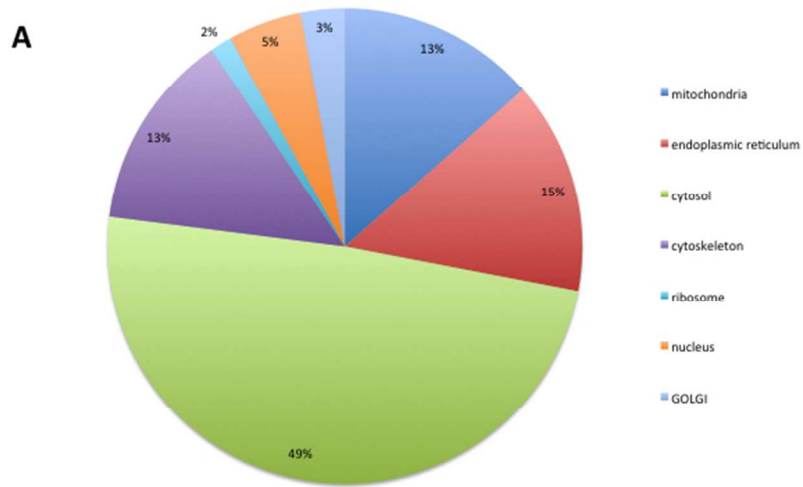


254x190mm (72 x 72 DPI)



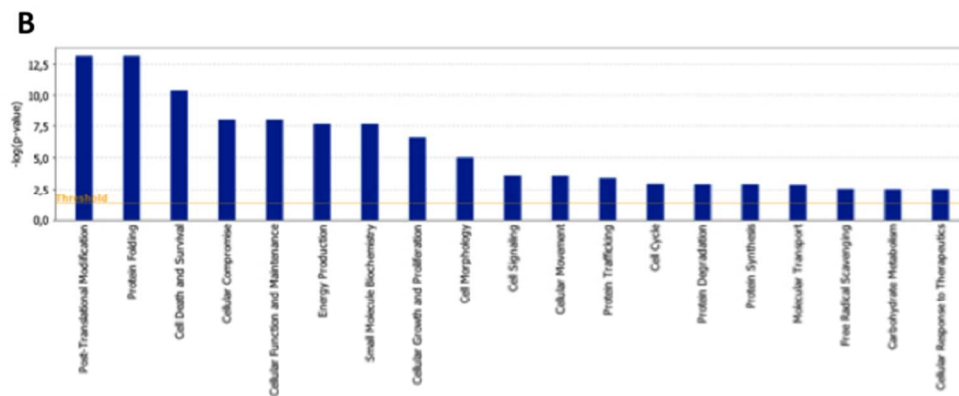
254x190mm (72 x 72 DPI)

Figure 7A, Messina et al



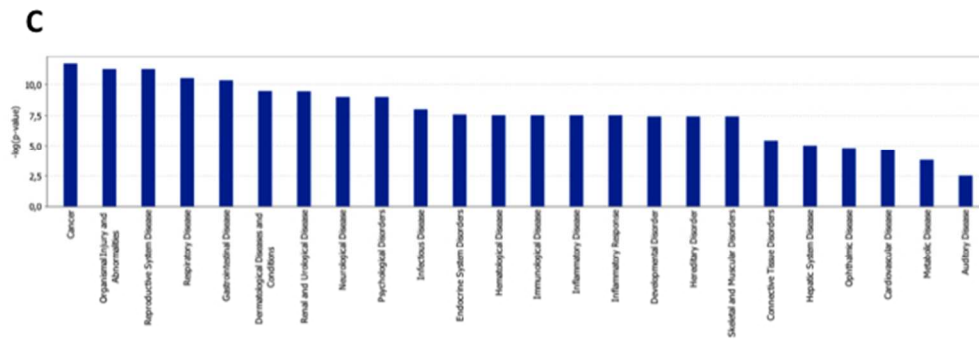
254x190mm (72 x 72 DPI)

Figure 7B, Messina et al



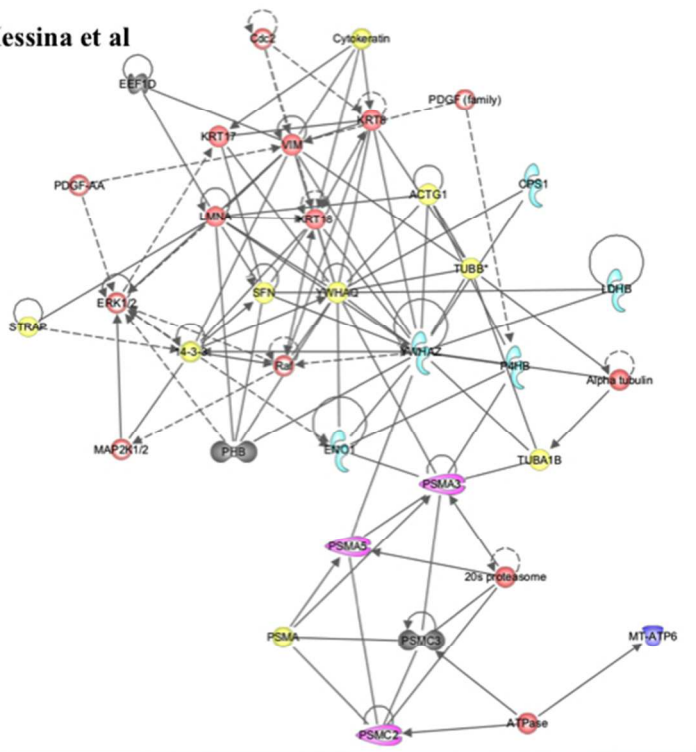
254x190mm (72 x 72 DPI)

Figure 7C, Messina et al



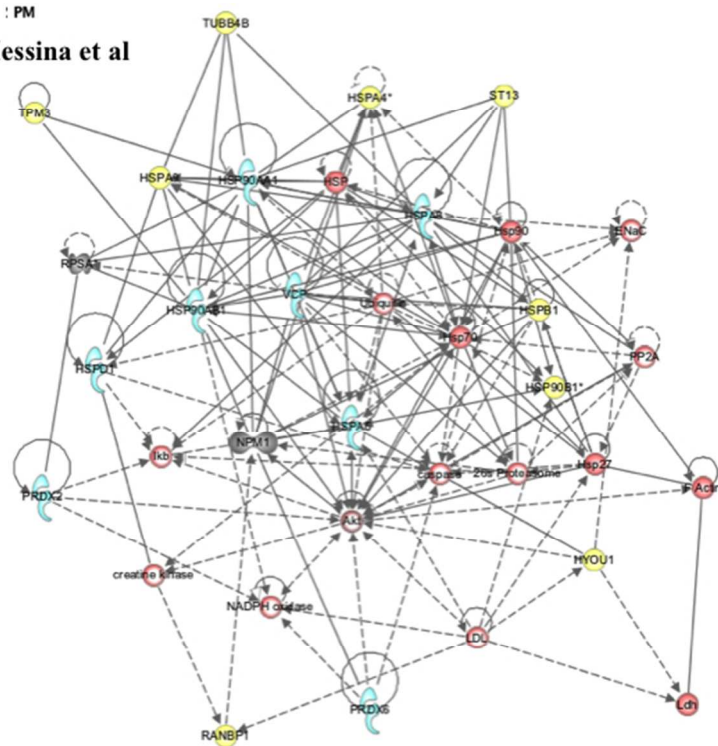
254x190mm (72 x 72 DPI)

Figure 8A, Messina et al



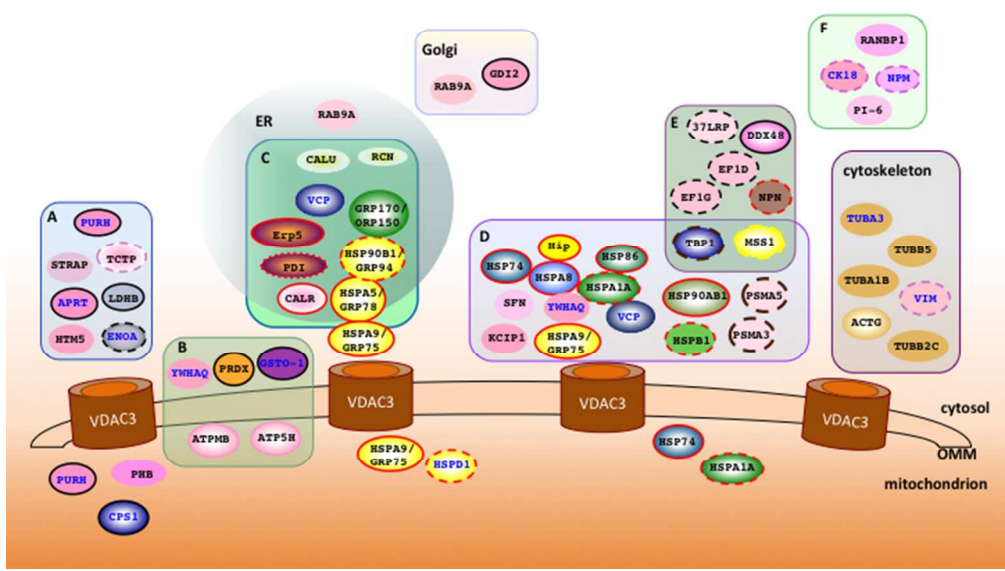
254x190mm (72 x 72 DPI)

Figure 8B, Messina et al



254x190mm (72 x 72 DPI)

Figure 9, Messina et al.



254x190mm (72 x 72 DPI)